

Junction Temperature Estimation of IGBT Based Inverter Using Kalman Filter

¹Amal Sasi, ² Uma Symkumar

¹Dept. of Electrical Engineering Govt. Engineering College, Thrissur, Kerala, India

² Dept. of Electrical Engineering Govt. Engineering College, Thrissur, Kerala, India

E-mail: ¹ amalsasi@outlook.com, ² uma@gectcr.ac.in

ABSTRACT

Thermal stress due to varying load in power electronic converters leads to power module failure. To prevent the failure due to thermal stress proper health management is provided based on the temperature value. Thus, accurate knowledge of junction temperature is required. Temperature measurement using thermal sensors increase the circuit complexity. On the other hand ageing effect and variable coolant rate are the limiting factors in equivalent RC thermal model. In the proposed method a Kalman filter is introduced to thermal state model along with the temperature measurements from the TSEPs to increase the accuracy of the temperature estimation. The temperature is extracted from measured $V_{CE(on)}$, which is a temperature dependent quantity is used as the measured quantity in the Kalman filter. The filter updates the state variable by using the knowledge from measured quantity. The adaptivity of Kalman Filter gives the accurate estimation with the presence of error due to ageing, variable coolant rates and noise in the measurement of TSEPs. The algorithm is implemented in an H-bridge inverter with IGBT-IRG4BC40SPbF and the results are analyzed.

Keywords: Cross-coupling effects, H-bridge inverter Insulated Gate Bipolar Transistor (IGBT), Kalman Filter, Power loss model, Thermal model

1. INTRODUCTION

Due to increased power handling capability of semiconductor devices, power converters finds application in high power industries like the automobile industry, aerospace and utility grid. IGBT based power modules are best suitable for power equipment operating at medium power applications with high switching frequencies. The high current and larger power density generate a considerable amount of heat in the IGBT. The thermal stress produced by varying load condition reduces the lifetime and reliability and can damage the solder joints and the IGBT junction[1]. The accurate knowledge is vital for finding the remaining lifetime estimation [2] and to provide a control mechanism by reducing the switching frequency or by limiting the current[3]. The temperature measurement methods are basically of three types[4]. First one is the optical method which includes measurement using infrared cameras, infrared microscope and optical fibres. The optical method has a large time constant of approximately 25ms. The next method is the physical contact method, which includes NTCs and on-chip diode sensor. Integrating Negative Temperature Coefficient(NTC) resistors and on-chip diode sensors with the power module give

temperature information with a time constant of a few milliseconds. Disadvantages of these methods are requirements of additional pins, separate copper traces and might require special consideration for isolation from HV side. Another method is the extracting temperature from Thermosensitive Electrical Parameters (TSEPs). Intermittency and noise in the measurement of TSEPs are the main drawbacks of this method. Using thermal models such as an equivalent RC network are the simple and efficient method to estimate the junction temperature T_j . Ageing effect and variable coolant rate are the drawbacks of this method.

Physical method requires additional manufacturing design, that increases complexity. The last method is called an electrical method, includes use of TSEPs and RC equivalent thermal model. Temperature dependent electrical parameters are

- Gate threshold and gate turn off voltage V_{Gsth} .
- Saturation current I_{sat} .

- Short-circuit current I_{sc} .
- Turn on delay time, turn off time and turn off delay time.

- Current change rate and voltage change rate.
- Peak gate current I_G .

The measurement of these parameters requires high precision sensors and extra circuitry. The most common TSEP used for temperature is on state voltage drop $V_{CE(on)}$ [5]. The resulting $V_{CE(on)}$ measurement is translated into junction temperature T_j using mathematical formula or from a look-up table. Due to the inaccuracies and low sensitivity of $V_{CE(on)}$ measurement, the junction temperature T_j also becomes noisy. In order to eliminate the intermittency and noise, Kalman Filter [6] is introduced. Kalman filter is constructed as a mean square minimizer that uses state model of heat conduction path and the temperature measurement from VCE as shown in fig.1. In state model the power loss calculated from the current is as given input and junction temperature T_j is the output. The adaptive property of Kalman filter follows an accurate and consistent estimates of junction temperature T_j in presences of ageing effects, variable coolant flows and intermittency and noise in the measurement

2. POWER LOSS MODEL

Conduction loss and switch loss are major losses in the IGBT. These losses dissipate as heat, which increases the junction

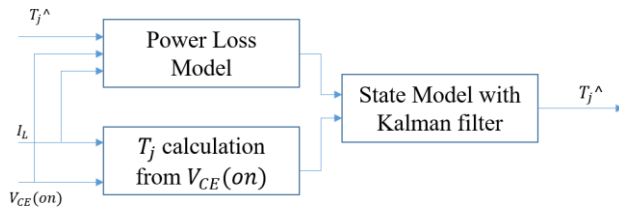


Fig.1. Block diagram of junction temperature using Kalman Filter.

temperature. The heat flow from the junction to ambient is shown as Fig. 2. In the thermal equivalent electrical network, the power loss of an IGBT or a diode chip is analogous to a current source. Thermal capacity and thermal resistance are equivalent to a capacitor and a resistor respectively. The thermal equivalent circuit is obtained by employing either the Cauer Model or Foster Model. Foster model as shown in fig.3 is employed here due to its simplicity. In order to introduce the Kalman filter RC network is converted into State Space model.

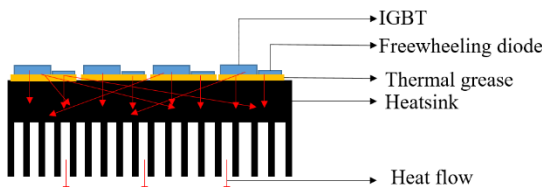


Fig. 2. Heat flow from junction to ambient.

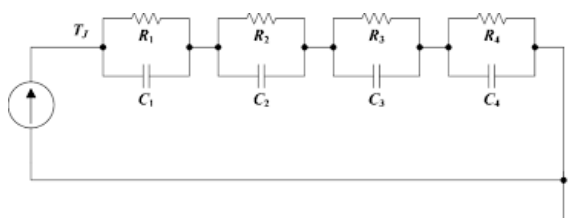


Fig. 3. Foster Network

2.1. Calculation of Conduction loss: The instantaneous conduction loss is obtained by multiplying the instantaneous voltage drop across the device during the ON state and current.

$$P_{cond} = V_{ce}(t) * I_c(t) \quad (1)$$

On state voltage drop VCE is measured to calculate the conduction loss and as a TSEP. The conduction loss of antiparallel diode is calculated as

$$P_{diode} = I_d * R_f \quad (2)$$

The forward resistance Rf of diode is dependent on the temperature.

2.2. Switching Loss: The switching loss is found by multiplying switching off (E_{off}) and on (E_{on}) energy with frequency(3).

$$P_{sw} = (E_{on} + E_{off}) * f_{sw} \quad (3)$$

The power electronics manufacturer itself provide the information of switching energies. If not, it can be found from turn off and turn on delay. From the power module data-sheet it is seen that the switching energies depend on the junction temperature (Tj).

2.3. Cross-Coupling effects: The heat flow from any device dissipating power to ambient through coolant

give rise to increased temperature not just at the device dissipating but at all other points in the module[7]. Usually FEM tool is used to find the cross-coupling effects between different different heat dissipating sources. Here cross-coupling effects is found by experimental methods. For finding the self the effects, the device under test is loaded with a constant current sufficient to rise a temperature and the cooling curves is obtained by plotting the thermal impedance Z_{Th} as in (4) v/s time.

$$Z_{TH}(t) = \frac{T_j(t) - T_a(t)}{P} = \frac{\Delta T_{ja}(t)}{P} \quad (4)$$

For measuring the cross coupling effects, the constant power loss is given to the neighbouring of the power module and the junction temperature of the device under test is measured and cooling curves are obtained. Similar configurations are used to find other self and cross heating effects.

2.4. State Space Modelling: The time response of the Foster network is described by a series of exponential terms of as in (5) .By taking the Laplace transform of (4) gives in to frequency domain and expressed as partial fraction (6).

$$Z_{TH}(t) = \sum_{i=1}^n R_i \left(1 - e^{-\frac{t}{\tau}} \right) \quad (5)$$

$$Z_{th}(s) = \frac{k_1}{s+p_1} + \frac{k_2}{s+p_2} + \frac{k_3}{s+p_3} + \dots + \frac{k_n}{s+p_n} \quad (6)$$

where k_i and p_i are the residues and poles of the transfer function, respectively, and s is the complex variable. By algebraic manipulation, it can be found that poles and residues are related to the RC components by the following formulas:

$$K_i = \frac{1}{C_i} \text{ \& } P_i = R_i C_i$$

These R and C values has no correlation with physical structure. These parameters only fit the temperature characteristics. The discrete state-space considering the self-heating and cross coupling effects with sampling time T_s are shown as in (7)

The thermal path between junction to ambient is represented in the state space form with Power loss as the input and Tj as the output. The states of the model is nodal voltage in the Foster network. In (7) a second order Foster network is used to represents the self-heating effects and first order Foster is used to represent the cross-coupling effects.

$$\begin{bmatrix} x_1(k+1) \\ x_2(k+1) \\ x_3(k+1) \\ x_4(k+1) \end{bmatrix} = \begin{bmatrix} \frac{1}{R_1 C_1} T_s + 1 & 0 & 0 & 0 \\ 0 & \frac{1}{R_2 C_2} T_s + 1 & 0 & 0 \\ 0 & 0 & \frac{1}{R_3 C_3} T_s + 1 & 0 \\ 0 & 0 & 0 & \frac{1}{R_4 C_4} T_s + 1 \end{bmatrix} \begin{bmatrix} x_1(k) \\ x_2(k) \\ x_3(k) \\ x_4(k) \end{bmatrix} + \begin{bmatrix} \frac{1}{C_1} T_s & 0 \\ \frac{1}{C_2} T_s & 0 \\ \frac{1}{C_3} T_s & 0 \\ \frac{1}{C_4} T_s & 0 \end{bmatrix} [P_{IGBT} \quad T_a]$$

$$T_j(k) = [1 \ 1 \ 1 \ 1] \begin{bmatrix} x_1(k) \\ x_2(k) \\ x_3(k) \\ x_4(k) \end{bmatrix} + [0 \ 1] [P_{IGBT} \quad T_a]$$

$x_1(k)$ & $x_2(k)$ are nodal voltages of equivalent circuit of self-effects. $x_3(k), x_4(k)$ & $x_5(k)$ are the nodal voltages of equivalent circuit of cross-heating effects of device 2, 3 and 4 respectively.

3. Introduction Of Kalman Filter In Temperature Estimation

Kalman filter accurately estimates the junction temperature utilizing the linear state model of the thermal path and junction temperature measured from VCE. The temperature calculation from the V_{CE} and the current is shown in fig. 4

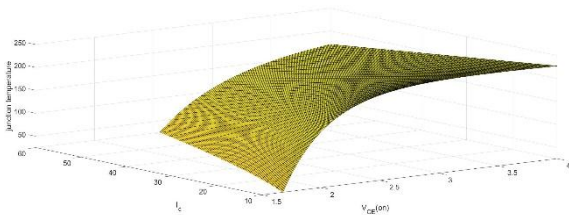


Fig. 4. Mathematical model for Tj of IGBT-IRG4BC40SPbF

The discrete state model of the thermal path with A and B as the state transition matrix and input matrix respectively, C and D are output matrix and feedforward matrix respectively is given as

$$x(k+1) = Ax(k) + Bu(k) + w(k) = f(x_k, u_k, w_k) \quad (8)$$

$$T_j(k) = Cx(k) + Du(k) + v_k \quad (9)$$

In (8) and (9) w_k and v_k are the noise matrix of state and output respectively. The covariance of these noise matrix are assumed stationary are given by

$$Q = E[w_k w_k^T] \quad (10)$$

$$R = E[v_k v_k^T] \quad (11)$$

The error co-variance matrix P_k is given by

$$P_k = E[e_k e_k^T] = E[(x_k - x'_k)(x_k - x'_k)^T] \quad (12)$$

With the Tj measurement $T_j(\text{meas})$, it is possible to update the state equation as

$$x'(k+1) = f(x'_k, u_k) + K_k(T_j(\text{meas}) - T'_j) \quad (13)$$

In (13) K_k is Kalman gain, which is derived in order to reduce the Mean Square Error (MSE), $x'(k+1)$ is new state estimate. The block diagram of Kalman filter is shown in fig. 5. The Kalman gain K_k is given by

$$K_k = P'_k H^T (H P'_k H^T + R)^{-1} \quad (14)$$

The update for the error covariance matrix P_k from the previous error covariance matrix P_k is given by

$$P'_k = (I - K_k H) P_k \quad (15)$$

In the proposed system the measured Tj is obtained from on

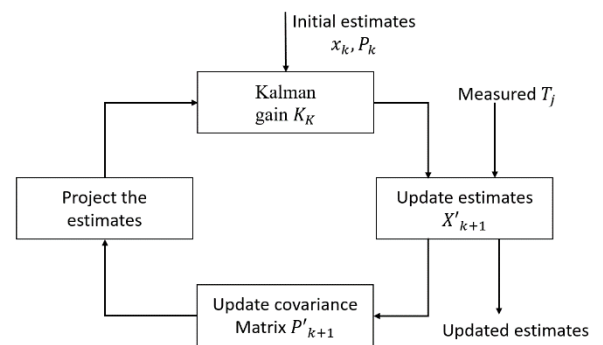


Fig. 5. Block diagram of Kalman filter

state voltage drop $V_{CE(\text{on})}$, which is available when switch is at ON state only. Thus Kalman operates in two modes prediction mode and correction mode. When the Tj is not available the Kalman predicts the Tj from the state model, that is the prediction mode. In correction mode the Kalman updates states using the Tj measured.

4. Experimental Setup

To validate the algorithm the H-bridge inverter with following specifications are used. The experimental set-up consists of H-bridge attached on a common heat sink as shown in fig. 6. The hardware set-up has provision to load IGBT individually and can measure VCE across each switches. The V_{CE} data and current data is logged through a data acquisition system. The temperature is estimated offline through Matlab.

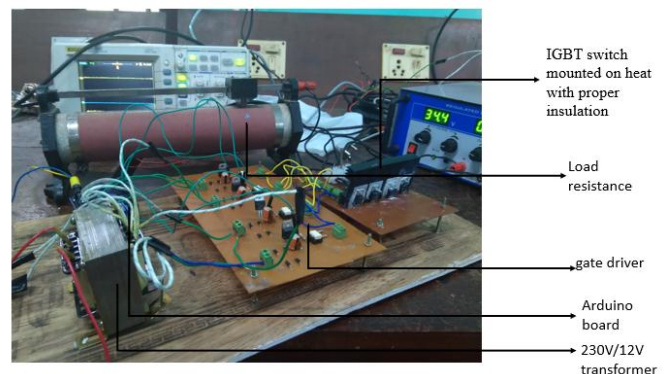


Fig. 6. Experimental set-up

TABLE I COMPONENTS USED

Components/ Parameters Selected	Rating
IGBT-IRG4BC40SPbF	600V, 31A

©2012-20 International Journal of Information Technology and Electrical Engineering

Switching frequency	10kHz
TIM	Mica sheet and Silica gel
Type of connection	Copper Cable
Heat sink	75mmx45mm with 4 fins

TABLE II RC PARAMETERS OF EQUIVALENT THERMAL NETWORK

R_{11}	0.18	R_{12}	4.185	R_2	1.57	R_3	.56	R_4	.56
C_{11}	3.88	C_{12}	0.99	C_2	0.99	C_3	2.6	C_4	3.8

A. RC parameters

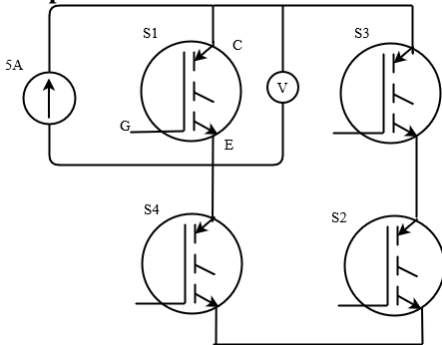


Fig. 7. Circuit Diagram to find Self-heating effects

As shown in fig. 7 the circuit diagram is find self-heating effect of IGBT S1. The S1 is loaded with 5A constant current for 10s and its corresponding VCE values are recorded. 5A is sufficient to raise the junction temperature. From the recorded VCE, the temperature is obtained from the look-up table. Selfheating transient impedance curve is calculated by dividing is the temperature rise with power loss. For finding the crosscoupling heating effects switch S1 is loaded with a small current and S4 is loaded with 5A and voltage across S1 is recorded as shown in fig.8. Cross-heating transient impedance curve is obtained from dividing the temperature rise of S1 obtained from the VCE recordings with power-loss of S4. Similarly, different circuit configurations are used to find all other cross-coupling effects. Using Matlab curve fitting tool RC parameter are fitted from the Foster equations. The RC parameters are listed in Table II. A second-order Foster

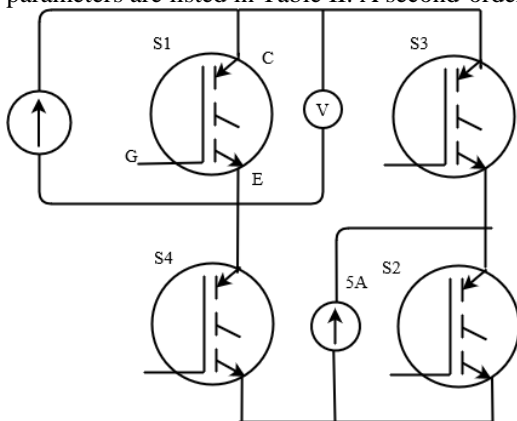


Fig. 8. Circuit Diagram to find Cross-coupling effect of S1 due to S4

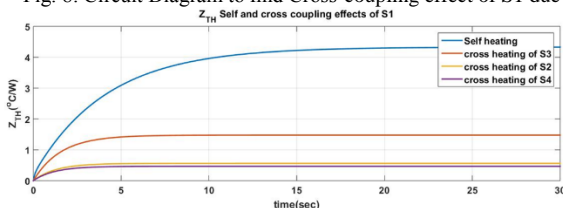


Fig. 9. Transient impedance curves for self and cross-coupling effects

network is used to fit the self-heating effects and first-order Foster for cross-coupling effects. RC parameters values are listed in table x and corresponding curves are shown in fig. 9

5. Results And Analysis

The H- bridge is loaded with a current of 4A. The VCE is obtained as shown in fig. 10, it is clear the VCE measurement contains intermittency and noise. These noises will result

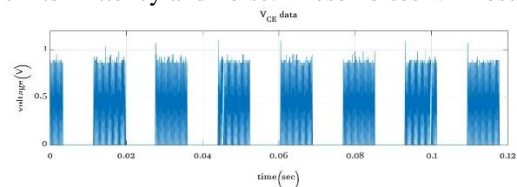


Fig. 10. Voltage waveform across the switch(VCE)

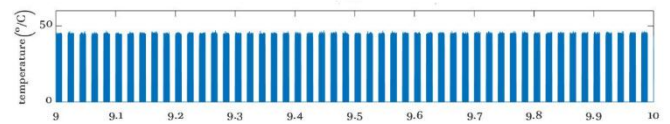


Fig. 11. Temperature value extracted from VCE(on) recordings

In the temperature obtained from the look-up table as shown in fig. 10. Fig. 11 shows the temperature value obtained from the state-space model. The state-space was made from temperature-independent RC parameters. Actually, the RC parameters change with temperature, coolant rates and ageing effects. There will be an error in temperature obtained from the state-space model. The kalman filter utilizes the advantage of both measurements and drawbacks. The temperature estimated temperature is shown in the fig. 12

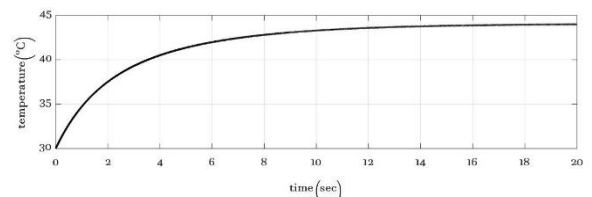


Fig. 12. Temperature from the State-Space model

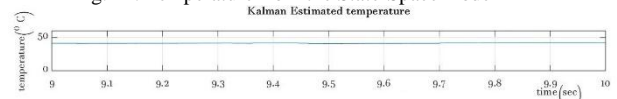


Fig. 13. Kalman Filter Estimated TjOutbreak

6. Conclusion

The estimation of junction temperature using Kalman filter is verified experimentally with single-phase H-bridge inverter with IGBT IRG4BC40SPbF. The thermal RC parameters are found experimentally and state-space model is found. Kalman Filter is applied to the State-space model with temperature measurements from the

$V_{CE(on)}$ data. Finally, the temperature is estimated accurately. Kalman Filter eliminates the noise and intermittency in the temperature measurement from $V_{CE(on)}$, also Kalman eliminates errors due to ageing and variable cooling conditions.

REFERENCES

- [1] M. Ciappa, "Selected failure mechanisms of modern power modules", *Microelectron. Rel.*, vol. 42, nos. 45, pp. 653667, Apr./May 2002.
- [2] H. Hui and P. A. Mawby, "A lifetime estimation technique for voltage source inverters", *IEEE Trans. Power Electron.*, vol. 28, no. 8, pp. 41134119, Aug. 2013.
- [3] Musallam, P.P.Acarney, C.M.Johnson ,L. Pritchard, and V. Pickert, "Estimation and control of power electronic device temperature during operation with variable conducting current", *IET Circuits, Devices Syst.*, vol. 1, pp. 16, 2007.
- [4] Mohamed Halick Mohamed Sathik, Josep Pou, Sundararajan Prasanth, Vivek Muthu, Rejeki Simanjorang and Amit Kumar Gupta "Comparison of IGBT junction temperature measurement and estimation methods-a review "2017 Asian Conference on Energy, Power and Transportation Electrification (ACEPT)., Year: 2017 Pages: 1 – 8
- [5] X. Perpi, J.-F. Serviere, J. Saiz, D. Barlini, M. Mermet-Guyennet, and J. Milln, "Temperature measurement on series resistance and devices in power packs based on on-state voltage drop monitoring at high current," *Microelectronics Reliability.*, vol. 46, pp. 1834-1839, Sep. 2006.
- [6] M. S. Grewal and A. P. Andrews, "Kalman Filtering: Theory and Practice Using MATLAB." New York, NY, USA: Wiley, 2011.
- [7] M. J. Whitehead, C. M. Johnson, "Junction Temperature Elevation as a Result of Thermal Cross Coupling in a Multi-Device Power Electronic Module" in *1st Electronic Systemintegration Technology Conference, 2006,pp.: 1218 - 1223*
- [8] Mohd. Amir Eleffendi ; C. Mark Johnson "Application of Kalman Filter to Estimate Junction Temperature in IGBT Power Modules " *IEEE Transactions on Power Electronics Year: 2016 — Volume: 31, Issue: 2*